Journal of Engineering and Natural Sciences
Mühendislik ve Fen Bilimleri Dergisi

Sigma 33, 200-218, 2015

Research Article / Araştırma Makalesi

FREE VIBRATION ANALYSIS OF HELICOIDAL BARS WITH THIN-WALLED CIRCULAR TUBE CROSS-SECTION VIA MIXED FINITE ELEMENT METHOD

Nihal ERATLI*, Merve ERMİŞ, Mehmet H. OMURTAG

Department of Civil Engineering, Istanbul Technical University, ISTANBUL

Received/Geliş: 22.01.2015 Revised/Düzeltme: 13.04.2015 Accepted/Kabul: 18.05.2015

ABSTRACT

In this study, the free vibration analysis of cylindrical and non-cylindrical helicoidal bars with thin-walled circular tube cross-section is investigated by using the mixed finite element formulation based on Timoshenko beam theory. Frenet triad is adopted as the local coordinate system in the helix geometry. The curved elements involve two nodes, where each node has 12 DOF, namely three translations, three rotations, two shear forces, one axial force, two bending moment and one torque. Numerical solutions are performed to analyze the dynamic behavior of the helix geometries and benchmark results are presented. Parametric studies are carried out to investigate the influence of the section geometry, the helicoidal geometry, the boundary conditions and the density of the material.
Keywords: Timoshenko beam theory, finite element, non-cylindrical helix, thin-walled circular tube section, free vibration.

İNCE CİDARLI DAİRESEL TÜP KESİTLİ HELİSEL ÇUBUKLARIN KARIŞIK SONLU ELEMAN YÖNTEMİYLE SERBEST TİTREŞİM ANALİZİ

ÖZET

Bu çalışmada, ince cidarlı tüp kesite sahip silindirik ve silindirik olmayan helisel çubukların serbest titreşimi Timoshenko çubuk kuramını esas alan bir karışık sonlu eleman formülasyonu kullanılarak incelenmiştir. Helis geometrisinde Frenet koordinat sistemi kullanılmıştır. İki düğüm noktalı eğrisel elemanın bir düğüm noktasında, üç yer değiştirme, üç dönme, iki kesme kuvveti, bir eksenel kuvvet, iki eğilme momenti ve bir burulma momenti olmak üzere, 12 bilinmeyen vardır. Helis geometrilerinin dinamik davranışı sayısal olarak incelenmiş ve literatüre özgün katkı sağlanmıştır. Kesit ve helis geometrileri, sınır koşulları ve malzeme yoğunluğu gibi parametrelerin etkisinin incelendiği parametrik çalışmalar yapılmıştır.
Anahtar Sözcükler: Timoshenko çubuk kuramı, sonlu eleman, silindirik olmayan helis, ince cidarlı tüp kesit, serbest titreşim.

1. INTRODUCTION

Derivation of the differential equations of helicoidal bars goes back to 19th century [1-3]. Shear influence and rotary inertia effects are investigated by [4] and [5] derived the dynamic equations.

* Corresponding Author/Sorumlu Yazar: e-mail/e-ileti: eratli@itu.edu.tr, tel: (212) 285 65 52

Natural frequencies of helicoidal bars depend on different parameters, and in order to address them various numerical methods were employed such as the finite element method [6-8], the transfer matrix method [9] which are the most popular ones. The transfer matrix method is intensively applied to dynamic analysis of cylindrical/non-cylindrical helical springs besides finite element method with circular and rectangular cross-sections by [10-14]. [15] employed the exact element method for the free vibration analysis of non-cylindrical helicoidal beams with circular and rectangular variable cross-sections. [16,17] applied the pseudospectral method to investigate the free vibration analysis of cylindrical and non-cylindrical helical springs with circular cross-sections. In this study, free vibration analysis of cylindrical, conical, barrel and hyperboloidal helices having thin-walled circular tube cross-section is performed via the mixed finite element method. The influence of some parameters (e.g., the thickness-to-section average radius ratio, the helix height-to-helix maximum radius ratio, various parameters of the non-cylindrical helicoidal geometry, boundary conditions, and the density of the material) on the fundamental natural frequency of helicoidal bars are investigated.

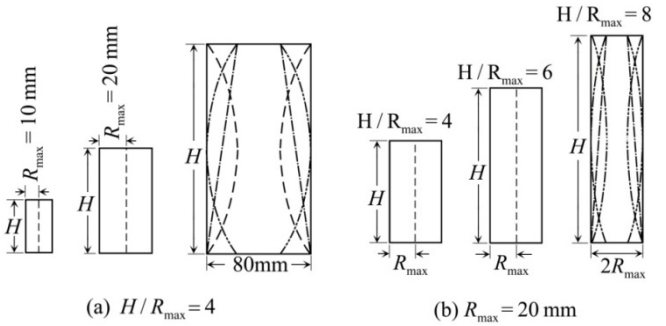

Figure 1. The envelope curves of helix geometries

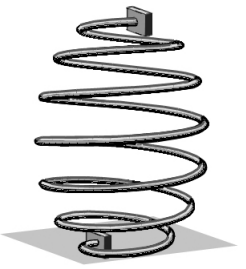

Figure 2. The barrel helix

2. THE HELIX GEOMETRY, THE FUNCTIONAL AND THE MIXED FINITE ELEMENT FORMULATION

Helix geometry: The geometrical properties of the helices in Figure 1 are $x = R(\varphi)\cos\varphi$, $y = R(\varphi)\sin\varphi$, $z = p(\varphi)\varphi$, $p(\varphi) = R(\varphi)\tan\alpha$, where α denotes the pitch angle, $R(\varphi)$ and $p(\varphi)$ signify the centerline radius and the step for unit angle, respectively, of the helix as a function of the horizontal angle φ. With $c(\varphi) = \sqrt{R^2(\varphi) + p^2(\varphi)}$, the infinitesimal arc length becomes $\mathrm{d}s = c(\varphi)\mathrm{d}\varphi$. In the cylindrical helix, since $R = R(\varphi) = \text{constant}$ and it is clear that $c = \sqrt{R^2 + p^2}$, $\chi = R/c^2$, $\tau = p/c^2$, $p = R\tan\alpha$ are all constant. χ and τ are the curvature and torsion of the helix axis, respectively. The Frenet unit vectors are as follows: $\mathbf{t}$ is the tangent unit vector, $\mathbf{n}$ is the normal unit vector, $\mathbf{b} = \mathbf{t} \times \mathbf{n}$ is the binormal unit vector. In the case of a conical helix, the radius at any point on the helix geometry is $R(\varphi) = R_{\max} + (R_{\min} - R_{\max})(\varphi/2n\pi)$ where n is the number of active turns, $R_{\max}$ and $R_{\min}$ are the bottom radius and top radius, respectively, of the conical helix geometry and in the case of a barrel, the radius is $R(\varphi) = R_{\max} + (R_{\min} - R_{\max})(1 - \varphi/n\pi)^2$, $R_{\min}$ and $R_{\max}$ are the bottom radius and the central radius, respectively or in the case of hyperboloidal helix, the radius is $R(\varphi) = R_{\min} + (R_{\max} - R_{\min})(1 - \varphi/n\pi)^2$, where $R_{\max}$ and $R_{\min}$ are the bottom radius and the central radius, respectively.

The functional: The field equations for the helicoidal bars, which are based on the Timoshenko beam theory and refer to the Frenet coordinate system, are discussed in [7,8]. Using $\mathbf{u}=u_t\,\mathbf{t}+u_n\,\mathbf{n}+u_b\,\mathbf{b}$ as the displacement vector, $\mathbf{\Omega}=\Omega_t\,\mathbf{t}+\Omega_n\,\mathbf{n}+\Omega_b\,\mathbf{b}$ as the rotational vector, $\mathbf{T}=T_t\,\mathbf{t}+T_n\,\mathbf{n}+T_b\,\mathbf{b}$ as the force vector, $\mathbf{M}=M_t\,\mathbf{t}+M_n\,\mathbf{n}+M_b\,\mathbf{b}$ as the moment vector, ρ as the density of material, A as the area of the cross-section, $\mathbf{I}$ as the moment of inertia, $\mathbf{q}$ and $\mathbf{m}$ as the distributed external force vector and moment vector, respectively, the field equations can be written in the form

$$\left.\begin{aligned} -\mathbf{T}_{,s}-\mathbf{q}+\rho A\,\ddot{\mathbf{u}}&=\mathbf{0}\\ -\mathbf{M}_{,s}-\mathbf{t}\times\mathbf{T}-\mathbf{m}+\rho\mathbf{I}\,\ddot{\mathbf{\Omega}}&=\mathbf{0}\end{aligned}\right\} \tag{1}$$

$$\left.\begin{aligned} \mathbf{u}_{,s}+\mathbf{t}\times\mathbf{\Omega}-\mathbf{C}_\gamma\mathbf{T}&=\mathbf{0}\\ \mathbf{\Omega}_{,s}-\mathbf{C}_\kappa\mathbf{M}&=\mathbf{0}\end{aligned}\right\} \tag{2}$$

where the accelerations are denoted by $\ddot{\mathbf{u}}=\partial^2\mathbf{u}/\partial t^2$, $\ddot{\mathbf{\Omega}}=\partial^2\mathbf{\Omega}/\partial t^2$. Eq. (1) is the equation of motion and Eq. (2) is the difference between the kinematic strain equation and the constitutive strain equation, namely, $\boldsymbol{\varepsilon}^{\mathbf{u}}-\boldsymbol{\varepsilon}^{\boldsymbol{\sigma}}=\mathbf{0}$. The kinematic strain equation is in form $\boldsymbol{\varepsilon}^{\mathbf{u}}=\mathbf{D}^k\mathbf{u}$, where $\mathbf{D}^k$ is a differential operator. The constitutive strain equation is in the form $\boldsymbol{\varepsilon}^{\boldsymbol{\sigma}}=\mathbf{C}\boldsymbol{\sigma}$, where $\mathbf{C}$ is the compliance matrix, namely,

$$\mathbf{C}_\gamma=\begin{bmatrix}1/EA & 0 & 0\\ 0 & 1/GA' & 0\\ 0 & 0 & 1/GA'\end{bmatrix},\ \mathbf{C}_\kappa=\begin{bmatrix}1/GI_t & 0 & 0\\ 0 & 1/EI_n & 0\\ 0 & 0 & 1/EI_b\end{bmatrix} \tag{3}$$

where $A'=A/k'$ and k' is the shear correction factor; E and G are the elasticity and shear modulus, respectively; I_t, I_n and I_b are the moments of inertia with respect to the t, n, b axes, respectively. Eqs. (1)-(2) can be written in operator form as $\mathbf{Q}=\mathbf{L}\mathbf{y}-\mathbf{f}$; if the operator is potential, the equality $\langle \mathrm{d}\mathbf{Q}(\mathbf{y},\bar{\mathbf{y}}),\mathbf{y}^*\rangle=\langle \mathrm{d}\mathbf{Q}(\mathbf{y},\mathbf{y}^*),\bar{\mathbf{y}}\rangle$ must be satisfied [18]. $\mathrm{d}\mathbf{Q}(\mathbf{y},\bar{\mathbf{y}})$ and $\mathrm{d}\mathbf{Q}(\mathbf{y},\mathbf{y}^*)$ are Gâteaux derivatives of the operator in the directions of $\bar{\mathbf{y}}$ and $\mathbf{y}^*$, respectively. After proving the operator to be potential and considering the harmonic motion of the helix in the free vibration analysis (and also $\mathbf{q}=\mathbf{m}=\mathbf{0}$), the functional yields to the following form

$$\begin{aligned}\mathbf{I}(\mathbf{y})=&-\left[\mathbf{u},\mathbf{T}_{,s}\right]+\left[\mathbf{t}\times\mathbf{\Omega},\mathbf{T}\right]-\left[\mathbf{M}_{,s},\mathbf{\Omega}\right]-\tfrac{1}{2}\left[\mathbf{C}_\kappa\mathbf{M},\mathbf{M}\right]-\tfrac{1}{2}\left[\mathbf{C}_\gamma\mathbf{T},\mathbf{T}\right]-\tfrac{1}{2}\rho A\omega^2\left[\mathbf{u},\mathbf{u}\right]\\ &-\tfrac{1}{2}\rho\omega^2\left[\mathbf{I}\mathbf{\Omega},\mathbf{\Omega}\right]+\left[\left(\mathbf{T}-\hat{\mathbf{T}}\right),\mathbf{u}\right]_\sigma+\left[\left(\mathbf{M}-\hat{\mathbf{M}}\right),\mathbf{\Omega}\right]_\sigma+\left[\hat{\mathbf{u}},\mathbf{T}\right]_\varepsilon+\left[\hat{\mathbf{\Omega}},\mathbf{M}\right]_\varepsilon\end{aligned} \tag{4}$$

where ω is the natural circular frequency and the square parentheses indicate the inner product. The terms with hats in Eq. (4) are known values on the boundary and the subscripts ε and σ represent the geometric and the dynamic boundary conditions, respectively.

The curved element: Using the subscripts i,j to represent the node numbers of the bar element, the linear shape functions $\phi_i=(\varphi_j-\varphi)/\Delta\varphi$ and $\phi_j=(\varphi-\varphi_i)/\Delta\varphi$ are employed in the finite element formulation, where $\Delta\varphi=(\varphi_j-\varphi_i)$. The non-cylindrical helix geometry is interpolated from the cylindrical geometry as stated by [7].

The free vibration analysis: The problem of determining the natural frequencies of a structural system reduces to the solution of a standard eigenvalue problem $([\mathbf{K}]-\omega^2[\mathbf{M}])\{\mathbf{u}\}=\{\mathbf{0}\}$ where $[\mathbf{K}]$ is the system matrix, $[\mathbf{M}]$ is the mass matrix for the entire domain, $\mathbf{u}$ is the eigenvector

and ω is the natural angular frequency of the system. Hence the explicit form of standard eigenvalue problem in the mixed formulation is

$$\left(\begin{bmatrix} [\mathbf{K}_{11}] & [\mathbf{K}_{12}] \\ [\mathbf{K}_{22}] & [\mathbf{K}_{22}] \end{bmatrix} - \omega^2 \begin{bmatrix} [\mathbf{0}] & [\mathbf{0}] \\ [\mathbf{0}] & [\mathbf{M}] \end{bmatrix} \right) \begin{Bmatrix} \{\mathbf{F}\} \\ \{\mathbf{U}\} \end{Bmatrix} = \begin{Bmatrix} \{\mathbf{0}\} \\ \{\mathbf{0}\} \end{Bmatrix} \tag{5}$$

where $\{\mathbf{F}\}$ denotes the nodal force and the moment vectors and $\{\mathbf{U}\} = \{\mathbf{u}\ \boldsymbol{\Omega}\}^T$ signifies the nodal displacement and rotation vectors. The $\{\mathbf{F}\}$ vector is eliminated in Eq. (5) and the eigenvalue problem in the mixed formulation becomes $([\mathbf{K}^*] - \omega^2[\mathbf{M}])\{\mathbf{U}\} = \{\mathbf{0}\}$ where the condensed system matrix is $[\mathbf{K}^*] = [\mathbf{K}_{22}] - [\mathbf{K}_{12}]^T [\mathbf{K}_{11}]^{-1} [\mathbf{K}_{12}]$.

3. NUMERICAL EXAMPLES

3.1. Convergence analysis

A barrel helix bar, having circular cross section and fixed at both ends is solved [see Figure 2]. The material and geometrical properties are: the modulus of elasticity $E = 210\,\text{GPa}$; Poisson's ratio $\upsilon = 0.3$; the material density $\rho = 7850\,\text{kg/m}^3$; the number of active turns $n = 6.5$; the pitch angle $\alpha = 4.8°$; the ratio of the minor radius to the major radius of the helix $R_{\min} / R_{\max} = 0.4$ (where $R_{\max} = 25\,\text{mm}$), radius of the circular cross section $r = 1\,\text{mm}$. Through the analysis, the first two natural frequencies of the barrel helix are calculated using 50, 75 and 100 mixed finite elements. The convergence of the first two frequencies compared with [12,17] and SAP2000, and the results are shown graphically in Figure 3. SAP2000 needs more than 500 elements for fulfillment but the result of 500 seems to be satisfactory. In this example, the shear correction factor $k' = 1.18$ is used [19] but [12,17] considered the value of shear correction factor as $k' = 1.1$.

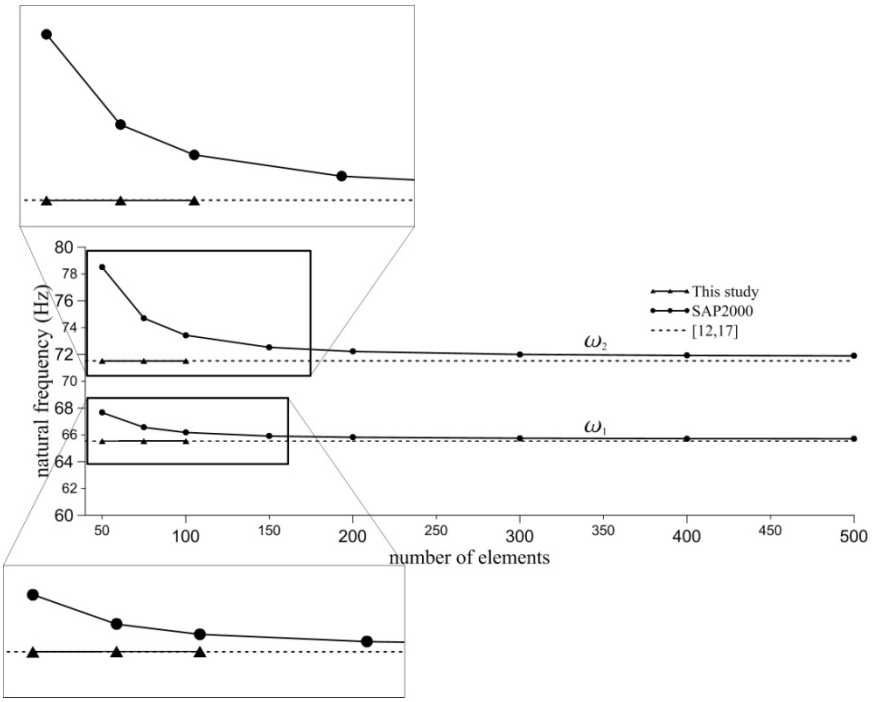

Figure 3. The first two frequencies graph for the barrel helix

3.2. Benchmark Examples

The material and geometrical properties of the cylindrical and non-cylindrical (conical, barrel, hyperboloidal) helicoidal bars, which are solved here, are as follows: the modulus of elasticity $E = 210\,\text{GPa}$; Poisson's ratio $\upsilon = 0.3$; the density of the material $\rho = 7850\,\text{kg/m}^3$; the number of active turns n (3.5, 7.5, 11.5); the minimum radius of helix-to-maximum radius of helix ratios $R_{\min} / R_{\max}$ (0.4, 0.6, 0.8); the height of helix-to-maximum radius of helix ratio $H / R_{\max}$ (4, 6, 8); the average radius of cross-section $r_o = 1\,\text{mm}$ is kept constant; and the thickness-to-cross-section average radius ratios t/r_o = 0.01, 0.10, 0.15 and 0.25. The pitch angle α has a unique value that refers to the number of active turns n and the ratios $R_{\min} / R_{\max}$ and $H / R_{\max}$ as shown in Table 1. In these examples, some cited parameters are kept constant for the solution, 200 mixed elements are employed.

3.2.1. Fixed-fixed Boundary Condition

$H / R_{\max} = 4 = \text{constant}$ [see Figure 1(a)]: The fundamental natural frequencies are listed in Tables 2(a)-(c). An interpretive discussion of each table is as follows: As the thickness-to-section average radius ratio increases, an increasing trend is observed for the fundamental natural frequency. For the thin-walled circular tube sections $(t / r_o \le 0.1)$, this increasing trend is nearly negligible. If the fundamental natural frequency values of each table are compared with the results that correspond to $t / r_o = 0.01$ for each helix type, the percent increase in the fundamental natural frequency, which corresponds to $t / r_o = 0.25$ for $R_{\max} = 10\,\text{mm}$, $20\,\text{mm}$

and $R_{\max} = 40\,\text{mm}$, ranges from $0.70\% \sim 0.87\%$ and $0.48\% \sim 1.06\%$, respectively. If the fundamental natural frequencies in each table are compared with the results that correspond to $n = 3.5$ for each helix type, the percent reduction in the case of $n = 7.5$ and $n = 11.5$ range between $46\% \sim 52\%$ and $64\% \sim 69\%$, respectively. If the fundamental natural frequencies of the non-cylindrical helices are compared with the fundamental natural frequencies of the cylindrical helix, the latter is smaller. For each number of turns, the comparison of the fundamental natural frequencies in each table with the results that correspond to $R_{\min} / R_{\max} = 0.4$ for each helix type reveals that the percent reduction in the case of conical, barrel and hyperboloidal helices range from $14\% \sim 36\%$, $8\% \sim 22\%$ and $18\% \sim 40\%$, respectively. The comparison of the fundamental natural frequencies in Tables 2(b)-(c) are compared with the corresponding results of Table 2(a) for each helix type reveal that the percent reductions in Tables 2(b) and 2(c) are approximately 75% and 94%, respectively.

$R_{\max} = 20\,\text{mm}$=constant [see Figure 1(b)]: The fundamental natural frequencies for $H / R_{\max} = 6, 8$ are listed in Tables 3(a)-(b). The common evaluations of the fundamental natural frequencies in each Table 2(b) and Tables 3(a)-(b) are as follows: As the thickness-to-section average radius ratio increases, an increasing trend is observed for the fundamental natural frequency. For thin-walled circular tube sections $(t / r_o \leq 0.1)$, this increasing trend is nearly negligible. The comparison of the fundamental natural frequencies in each table with the results that correspond to the ratio $t / r_o = 0.01$ for each helix type indicates that the percent increases in the fundamental natural frequency, which correspond to $t / r_o = 0.25$ for $H / R_{\max} = 4, 6, 8$, range from $0.68\% \sim 0.95\%$. The comparison of the fundamental natural frequencies in each table with the results that correspond to $n = 3.5$ for each helix type indicates that the percent reduction in the case of $n = 7.5$ and $n = 11.5$ range from $45\% \sim 52\%$ and $63\% \sim 69\%$, respectively. The comparison of the fundamental natural frequencies of the non-cylindrical helices with the cylindrical helix reveals that the latter is always smaller. For each number of turns, the fundamental natural frequencies in Table 2(b) and Tables 3(a)-(b) are compared with the results that correspond to $R_{\min} / R_{\max} = 0.4$; in the cases of $R_{\min} / R_{\max} = 0.6, 0.8$, the percent reductions for the $H / R_{\max} = 4, 6, 8$ ratios are listed in Table 4. The fundamental natural frequencies shown in Tables 3(a)-(b) are compared with the corresponding values in Table 2(b) [for $H / R_{\max} = 4$], and the reduction in the fundamental natural frequencies for the cylindrical, conical, barrel and hyperboloidal helices are listed in Table 5.

Table 1. The pitch angles (α) of helix types for the number of active turns n and the ratios R_{min} / R_{max} and H / R_{max}

H / R_{max}	R_{min} / R_{max}	cylindrical			conical			barrel			hyperboloidal		
		α			α			α			α		
		n=3.5	n=7.5	n=11.5	n=3.5	n=7.5	n=11.5	n=3.5	n=7.5	n=11.5	n=3.5	n=7.5	n=11.5
4	0.4				14.57°	6.91°	4.52°	12.81°	6.06°	3.96°	16.86°	8.05°	5.27°
	0.6				12.81°	6.06°	3.96°	11.85°	5.60°	3.65°	13.93°	6.60°	4.32°
	0.8				11.43°	5.39°	3.52°	11.03°	5.20°	3.39°	11.85°	5.59°	3.65°
	1.0	10.31°	4.85°	3.17°	-	-	-	-	-	-	-	-	-
6	0.4				21.29°	10.31°	6.77°	18.83°	9.04°	5.93°	24.45°	11.98°	7.87°
	0.6				18.83°	9.04°	5.93°	17.47°	8.36°	5.47°	20.41°	9.85°	6.46°
	0.8				16.86°	8.05°	5.27°	16.30°	7.77°	5.08°	17.47°	8.36°	5.47°
	1.0	15.26°	7.26°	4.75°	-	-	-	-	-	-	-	-	-
8	0.4				27.46°	13.63°	8.99°	24.45°	11.98°	7.88°	31.23°	15.80°	10.46°
	0.6				24.45°	11.98°	7.89°	22.77°	11.08°	7.28°	26.38°	13.03°	8.59°
	0.8				22.01°	10.68	7.01°	21.29°	10.31°	6.77°	22.77°	11.08°	7.28°
	1.0	19.99°	9.64°	6.32°	-	-	-	-	-	-	-	-	-

Table 2. The fundamental natural frequencies (Hz) for $H / R_{\max} = 4 = \text{constant}$ and $R_{\max} = \text{variable}$

(a) $R_{\max} = 10\,\text{mm}$, $H = 40\,\text{mm}$

n	$R\min / R\max$	cylindrical				conical				barrel				hyperboloidal			
		t / r_c				t / r_c				t / r_c				t / r_c			
		0.01	0.10	0.15	0.25	0.01	0.10	0.15	0.25	0.01	0.10	0.15	0.25	0.01	0.10	0.15	0.25
3.5	0.4					1191.8	1193.3	1196.2	1201.1	988.4	989.7	991.2	996.1	1310.1	1311.7	1313.9	1320.4
	0.6					1016.7	1017.9	1019.5	1024.6	904.2	905.4	906.8	906.8	1073.1	1074.4	1076.1	1081.5
	0.8					845.7	846.7	848.1	852.3	804.5	805.5	806.8	810.8	872.7	873.8	875.2	879.6
	1.0	696.2	696.9	698.0	701.5	-	-	-	-	-	-	-	-	-	-	-	-
7.5	0.4					632.9	633.7	634.7	637.8	500.8	501.4	502.2	504.7	689.4	690.2	691.3	694.8
	0.6					515.1	515.7	516.5	519.1	454.9	455.5	546.2	458.5	539.3	539.9	540.8	543.5
	0.8					412.0	412.5	413.2	415.3	395.4	395.9	396.6	398.5	423.1	423.6	424.3	426.4
	1.0	335.0	335.4	336.0	337.7	-	-	-	-	-	-	-	-	-	-	-	-
11.5	0.4					421.0	421.5	422.2	424.3	330.3	330.7	331.2	332.8	453.8	454.3	455.1	457.4
	0.6					338.9	339.3	339.8	341.6	300.5	300.9	301.4	302.9	352.3	352.7	353.3	355.1
	0.8					269.9	270.2	270.6	272.0	259.7	260.0	260.4	261.7	276.4	276.7	277.2	278.6
	1.0	219.2	219.5	219.8	220.9	-	-	-	-	-	-	-	-	-	-	-	-

Table 2 continuing…

(b) $R_{max} = 20\,\text{mm}$, $H = 80\,\text{mm}$

n	R_{min}/R_{max}	cylindrical				conical				barrel				hyperboloidal			
		t/r_c				t/r_c				t/r_c				t/r_c			
		0.01	0.10	0.15	0.25	0.01	0.10	0.15	0.25	0.01	0.10	0.15	0.25	0.01	0.10	0.15	0.25
3.5	0.4					299.7	300.1	300.6	302.1	247.9	248.2	248.6	249.8	330.0	330.4	331.0	332.6
	0.6					255.8	256.1	256.5	257.7	227.0	227.2	227.6	228.7	270.2	270.5	271.0	272.3
	0.8					212.9	213.1	213.5	214.5	202.3	202.6	202.9	203.9	219.7	220.0	220.3	221.4
	1.0	175.1	175.3	175.6	176.5	-	-	-	-	-	-	-	-	-	-	-	-
7.5	0.4					159.4	159.6	159.8	160.6	125.4	125.6	125.8	126.4	174.1	174.3	174.6	175.5
	0.6					130.2	130.4	130.6	131.2	114.1	114.2	114.4	114.9	136.2	136.4	136.6	137.3
	0.8					103.9	104.1	104.2	104.7	99.7	99.8	100.0	100.5	106.7	106.8	107.0	107.5
	1.0	84.4	84.5	84.6	85.0	-	-	-	-	-	-	-	-	-	-	-	-
11.5	0.4					106.1	106.2	106.4	106.9	82.7	82.8	82.9	83.3	114.6	114.8	115.0	115.6
	0.6					85.7	85.8	86.0	86.4	75.3	75.4	75.5	75.9	89.0	89.1	89.2	89.7
	0.8					68.1	68.2	68.3	68.6	65.5	65.6	65.7	66.0	69.7	69.8	69.9	70.3
	1.0	55.2	55.3	55.4	55.6	-	-	-	-	-	-	-	-	-	-	-	-

Table 2 continuing…

(c) $R_{\max} = 40\,\text{mm}$, $H = 160\,\text{mm}$

n	$R\min / R\max$	cylindrical				conical				barrel				hyperboloidal			
		t / r_c				t / r_c				t / r_c				t / r_c			
		0.01	0.10	0.15	0.25	0.01	0.10	0.15	0.25	0.01	0.10	0.15	0.25	0.01	0.10	0.15	0.25
3.5	0.4					75.0	75.1	75.3	75.6	62.0	62.1	62.2	62.5	82.7	82.8	82.9	83.3
	0.6					64.0	64.1	64.2	64.5	56.8	56.9	56.9	57.2	67.7	67.8	67.9	68.2
	0.8					53.3	53.4	53.5	53.7	50.7	50.7	50.8	51.0	55.0	55.1	55.2	55.4
	1.0	43.8	43.9	44.0	44.2	-	-	-	-	-	-	-	-	-	-	-	-
7.5	0.4					39.9	40.0	40.0	40.2	31.4	31.4	31.5	31.6	43.6	43.7	43.8	44.0
	0.6					32.6	32.7	32.7	32.9	28.5	28.6	28.6	28.8	34.1	34.2	34.2	34.4
	0.8					26.0	26.1	26.1	26.2	25.0	25.0	25.0	25.2	26.7	26.8	26.8	26.9
	1.0	21.1	21.2	21.2	21.3	-	-	-	-	-	-	-	-	-	-	-	-
11.5	0.4					26.6	26.6	26.6	26.8	20.7	20.7	20.7	20.8	28.8	28.8	28.8	29.0
	0.6					21.5	21.5	21.5	21.7	18.8	18.9	18.9	19.0	22.3	22.3	22.4	22.5
	0.8					17.1	17.1	17.1	17.2	16.4	16.4	16.5	16.5	17.5	17.5	17.5	17.6
	1.0	13.8	13.8	13.9	13.9	-	-	-	-	-	-	-	-	-	-	-	-

Table 3. The fundamental natural frequencies (Hz) for $R_{\max} = 20\,\text{mm} = \text{constant}$ and $H / R_{\max} = \text{variable}$

(a) $H / R_{\max} = 6$, $H = 120\,\text{mm}$

n	$R\min / R\max$	cylindrical				conical				barrel				hyperboloidal			
		t / r_c				t / r_c				t / r_c				t / r_c			
		0.01	0.10	0.15	0.25	0.01	0.10	0.15	0.25	0.01	0.10	0.15	0.25	0.01	0.10	0.15	0.25
3.5	0.4					242.3	242.6	243.0	244.2	215.5	215.8	216.1	217.2	265.8	266.1	266.5	267.8
	0.6					211.7	211.9	212.3	213.3	197.4	197.6	197.9	198.9	223.6	223.9	224.2	225.3
	0.8					184.1	184.3	184.6	185.5	178.7	179.0	179.2	180.1	188.7	189.0	189.3	190.2
	1.0	159.2	159.4	159.6	160.4	-	-	-	-	-	-	-	-	-	-	-	-
7.5	0.4					125.0	125.1	125.3	125.9	109.0	109.1	109.3	109.8	143.6	143.8	144.0	144.7
	0.6					107.2	107.4	107.5	108.1	98.8	98.9	99.1	99.5	116.5	116.6	116.8	117.4
	0.8					92.6	92.7	92.8	93.3	89.2	89.3	89.4	89.9	96.1	96.2	96.3	96.8
	1.0	80.2	80.3	80.4	80.8	-	-	-	-	-	-	-	-	-	-	-	-
11.5	0.4					82.7	82.8	82.9	83.3	71.9	72.0	72.1	72.4	95.8	95.9	96.1	96.6
	0.6					70.8	70.9	71.0	71.3	65.1	65.2	65.3	65.6	77.1	77.2	77.4	77.7
	0.8					61.0	61.1	61.2	61.5	58.8	58.8	58.9	59.2	63.4	63.5	63.6	63.9
	1.0	52.9	53.0	53.1	53.3	-	-	-	-	-	-	-	-	-	-	-	-

Table 3 continuing…
(b) $H / R_{\max} = 8$, $H = 160\,\text{mm}$

n	$R\min / R\max$	cylindrical				conical				barrel				hyperboloidal			
		t / r_c				t / r_c				t / r_c				t / r_c			
		0.01	0.10	0.15	0.25	0.01	0.10	0.15	0.25	0.01	0.10	0.15	0.25	0.01	0.10	0.15	0.25
3.5	0.4					190.7	190.9	191.2	192.2	170.0	170.2	170.5	171.4	209.4	209.7	210.0	211.0
	0.6					168.7	169.0	169.2	170.1	157.3	157.5	157.7	158.5	179.1	179.3	179.6	180.4
	0.8					149.3	149.4	149.7	150.4	144.7	144.8	145.1	145.8	153.5	153.7	154.0	154.7
	1.0	132.0	132.2	132.4	133.0	-	-	-	-	-	-	-	-	-	-	-	-
7.5	0.4					99.7	99.8	100.0	100.5	87.2	87.3	87.5	87.9	114.7	114.8	115.0	115.6
	0.6					86.4	86.5	86.7	87.1	79.7	79.8	79.9	80.3	93.9	94.0	94.1	94.6
	0.8					75.5	75.6	75.7	76.1	72.8	72.8	73.0	73.3	78.3	78.4	78.6	78.9
	1.0	66.3	66.4	66.5	66.9	-	-	-	-	-	-	-	-	-	-	-	-
11.5	0.4					66.2	66.3	66.4	66.7	57.7	57.8	57.9	58.2	76.8	76.9	77.0	77.4
	0.6					57.2	57.3	57.3	57.6	52.6	52.7	52.8	53.1	62.3	62.4	62.5	62.8
	0.8					49.8	50.0	50.0	50.2	48.0	48.1	48.1	48.4	51.8	51.8	51.9	52.2
	1.0	43.7	43.8	43.9	44.1	-	-	-	-	-	-	-	-	-	-	-	-

Table 4. The percent reductions in the fundamental natural frequencies of non-cylindrical helices in the case of $R_{min} / R_{max} = 0.6, 0.8$ with respect to $R_{min} / R_{max} = 0.4$.

H / R_{max}	Helix types		
	Conical	Barrel	Hyperboloidal
4	14% ~ 36%	8% ~ 21%	18% ~ 40%
6	12% ~ 27%	8% ~ 19%	15% ~ 34%
8	11% ~ 25%	7% ~ 17%	14% ~ 33%

Table 5. The percent reductions in the fundamental natural frequencies of cylindrical and non-cylindrical helices in the case of $H / R_{max} = 6, 8$ with respect to $H / R_{max} = 4$

H / R_{max}	n	Helix types			
		Cylindrical	Conical	Barrel	Hyperboloidal
6	3.5	9%	13% ~ 20%	11% ~ 13%	14% ~ 20%
	7.5	5%	10% ~ 22%	10% ~ 14%	9% ~ 18%
	11.5	4%	10% ~ 22%	10% ~ 14%	9% ~ 17%
8	3.5	25%	29% ~ 37%	28% ~ 32%	30% ~ 37%
	7.5	22%	27% ~ 38%	26% ~ 31%	26% ~ 35%
	11.5	21%	26% ~ 38%	26% ~ 31%	25% ~ 33%

3.2.2 The fixed-free Boundary Condition

$R_{max} = 20\,\text{mm} = \text{constant}$ [see Figure 1(b)]: The fundamental natural frequencies are shown in Tables 6(a)-(c), and the common evaluations are as follows: As the thickness-to-section average radius ratio increases, an increasing trend is observed for the fundamental natural frequency. In the case of $t / r_o = 0.01$ for each helix type for $t / r_o = 0.25$, the percent increase are shown in Table 7. The comparison of the fundamental natural frequency values in each table with the results that correspond to $n = 3.5$ for each helix type reveals that the percent reduction for $n = 7.5$ and $n = 11.5$ range from $48\% \sim 53\%$ and $65\% \sim 69\%$, respectively. The comparison of the fundamental natural frequency values for the non-cylindrical helices with the cylindrical helix reveals that the latter is smaller. For each number of turns, the fundamental natural frequency values in each table are compared with the results that correspond to $R_{min} / R_{max} = 0.4$; the percent reductions in $R_{min} / R_{max} = 0.6$ and 0.8 are listed in Table 8. The fundamental natural frequencies shown in Tables 6(b)-(c) are compared with the results in Table 6(a) [for $H / R_{max} = 4$], and the percent reduction in the fundamental frequency are listed in Table 9.

Table 7. The percent reductions in the fundamental natural frequencies of non-cylindrical helices in the case of $t / r_o = 0.25$ with respect to $t / r_o = 0.01$

H / R_{max}	Helix types			
	Cylindrical	Conical	Barrel	Hyperboloidal
4	0.68% ~ 0.89%	0.60% ~ 1.06%	0.53% ~ 1.16%	0.63% ~ 1.16%
6	0.00% ~ 0.63%	0.56% ~ 1.00%	0.00% ~ 1.01%	0.56% ~ 1.09%
8	0.81% ~ 1.27%	0.66% ~ 1.16%	0.00% ~ 1.18%	0.61% ~ 1.09%

Table 6. The fundamental natural frequencies (Hz) for $R_{\max} = 20\,\text{mm} = \text{constant}$ and $H / R_{\max} = \text{variable}$

(a) $H / R_{\max} = 6$, $H = 80\,\text{mm}$

n	$R\min / R\max$	cylindrical			conical			barrel			hyperboloidal		
		t / r_c			t / r_c			t / r_c			t / r_c		
		0.01	0.10	0.15	0.25	0.01	0.10	0.15	0.25	0.01	0.10	0.15	0.25
3.5	0.4					69.4	69.4	69.5	69.9	60.1	60.2	60.3	60.6	81.6	81.7	81.8	82.2
	0.6					60.6	60.7	60.8	61.1	55.4	55.5	55.5	55.8	66.8	66.9	67.0	67.3
	0.8					53.4	53.5	53.6	53.8	51.2	51.3	51.3	51.6	55.9	55.9	56.0	56.3
	1.0	47.4	47.5	47.6	47.8	-	-	-	-	-	-	-	-	-	-	-	-
7.5	0.4					33.4	33.4	33.4	33.6	28.7	28.7	28.8	28.9	39.5	39.5	39.6	39.8
	0.6					28.9	29.0	29.0	29.2	26.3	26.4	26.4	26.6	32.0	32.0	32.0	32.2
	0.8					25.4	25.4	25.4	25.6	24.3	24.3	24.4	24.5	26.5	26.6	26.6	26.7
	1.0	22.4	22.5	22.5	22.6	-	-	-	-	-	-	-	-	-	-	-	-
11.5	0.4					21.8	21.9	21.9	22.0	18.8	18.8	18.8	18.9	25.9	25.9	26.0	26.1
	0.6					18.9	19.0	19.0	19.1	17.2	17.2	17.3	17.4	20.9	20.9	21.0	21.1
	0.8					16.6	16.6	16.6	16.7	15.9	15.9	15.9	16.0	17.3	17.4	17.4	17.5
	1.0	14.7	14.7	14.7	14.8	-	-	-	-	-	-	-	-	-	-	-	-

Table 6. continuing…
(b) $H / R_{\max} = 6$, $H = 120\,\text{mm}$

n	$R\min / R\max$	cylindrical				conical				barrel				hyperboloidal			
		t / r_c				t / r_c				t / r_c				t / r_c			
		0.01	0.10	0.15	0.25	0.01	0.10	0.15	0.25	0.01	0.10	0.15	0.25	0.01	0.10	0.15	0.25
3.5	0.4					46.5	46.6	46.7	46.9	41.0	41.1	41.1	41.3	53.7	53.7	53.8	54.1
	0.6					41.1	41.2	41.3	41.5	38.0	38.1	38.1	38.3	44.8	44.9	44.9	45.2
	0.8					36.7	36.7	36.8	37.0	35.3	35.4	35.4	35.6	38.1	38.2	38.3	38.4
	1.0	33.0	33.0	33.1	33.2	-	-	-	-	-	-	-	-	-	-	-	-
7.5	0.4					22.9	22.9	23.0	23.1	19.9	20.0	20.0	20.1	26.8	26.8	26.9	27.0
	0.6					20.0	20.0	20.1	20.2	18.4	18.4	18.4	18.5	21.9	22.0	22.0	22.1
	0.8					17.7	17.7	17.7	17.8	17.0	17.0	17.1	17.1	18.4	18.5	18.5	18.6
	1.0	15.8	15.8	15.9	15.9	-	-	-	-	-	-	-	-	-	-	-	-
11.5	0.4					15.1	15.1	15.1	15.2	13.1	13.1	13.1	13.2	17.7	17.7	17.7	17.8
	0.6					13.1	13.2	13.2	13.2	12.1	12.1	12.1	12.1	14.4	14.4	14.5	14.5
	0.8					11.6	11.6	11.6	11.7	11.1	11.2	11.2	11.2	12.1	12.1	12.1	12.2
	1.0	10.4	10.4	10.4	10.4	-	-	-	-	-	-	-	-	-	-	-	-

Table 6. continuing…
(c) $H / R_{\max} = 8$, $H = 160\,\text{mm}$

n	$R\min / R\max$	cylindrical				conical				barrel				hyperboloidal			
		t / r_c				t / r_c				t / r_c				t / r_c			
		0.01	0.10	0.15	0.25	0.01	0.10	0.15	0.25	0.01	0.10	0.15	0.25	0.01	0.10	0.15	0.25
3.5	0.4					33.9	34.0	34.0	34.2	30.3	30.3	30.4	30.5	38.5	38.6	38.6	38.8
	0.6					30.3	30.4	30.4	30.6	28.2	28.3	28.3	28.4	32.7	32.8	32.8	33.0
	0.8					27.3	27.3	27.4	27.5	26.4	26.4	26.5	26.6	28.3	28.3	28.4	28.5
	1.0	24.7	24.8	24.8	24.9	-	-	-	-	-	-	-	-	-	-	-	-
7.5	0.4					17.2	17.3	17.3	17.4	15.1	15.1	15.1	15.2	20.0	20.1	20.1	20.2
	0.6					15.1	15.1	15.2	15.2	14.0	14.0	14.0	14.1	16.5	16.5	16.6	16.6
	0.8					13.4	13.5	13.5	13.5	13.0	13.0	13.0	13.1	14.0	14.0	14.0	14.1
	1.0	12.1	12.1	12.1	12.2	-	-	-	-	-	-	-	-	-	-	-	-
11.5	0.4					11.4	11.4	11.4	11.5	10.0	10.0	10.0	10.0	13.3	13.3	13.4	13.4
	0.6					10.0	10.0	10.0	10.1	9.2	9.2	9.2	9.3	10.9	10.9	10.9	11.0
	0.8					8.8	8.9	8.9	8.9	8.5	8.5	8.5	8.6	9.2	9.2	9.2	9.3
	1.0	7.9	7.9	7.9	8.0	-	-	-	-	-	-	-	-	-	-	-	-

Table 8. The percent reductions in the fundamental natural frequencies of non-cylindrical helices in the case of $R_{min} / R_{max} = 0.6, 0.8$ with respect to $R_{min} / R_{max} = 0.4$

H / R_{max}	Helix types		
	Conical	Barrel	Hyperboloidal
4	$12\% \sim 24\%$	$7\% \sim 16\%$	$18\% \sim 33\%$
6	$11\% \sim 23\%$	$7\% \sim 16\%$	$16\% \sim 32\%$
8	$10\% \sim 23\%$	$6\% \sim 15\%$	$14\% \sim 31\%$

Table 9. The percent reductions in the fundamental natural frequencies of cylindrical and non-cylindrical helices in the case of $H / R_{max} = 6, 8$ with respect to $H / R_{max} = 4$

H / R_{max}	Helix types			
	Cylindrical	Conical	Barrel	Hyperboloidal
6	$29\% \sim 31\%$	$30\% \sim 33\%$	$29\% \sim 32\%$	$30\% \sim 35\%$
8	$45\% \sim 48\%$	$46\% \sim 51\%$	$46\% \sim 50\%$	$46\% \sim 53\%$

3.2.3. Influence of Density on the Fundamental Natural Frequency

The thickness-to-section average radius ratio $t / r_o = 0.10 = \text{constant}$; the helix height to helix maximum radius ratio $H / R_{max} = 4 = \text{constant}$, where $R_{max} = 20\,\text{mm}$; and the densities of material $\rho = 7850\,\text{kg/m}^3$ and $8300\,\text{kg/m}^3$. The fundamental natural frequency results of the fixed-fixed and fixed-free boundary conditions are provided in Table 10(a) and Table 10(b), respectively. For the both boundary conditions, the percent reduction in the fundamental natural frequency values that correspond to $8300\,\text{kg/m}^3$ with respect to the corresponding results of $\rho = 7850\,\text{kg/m}^3$ range from $2.3\% \sim 3.2\%$.

Table 10. The fundamental natural frequencies (Hz) for two different density of material
(a) B.C. (boundary condition): fixed-fixed ($R_{max} = 20\,\text{mm}$, $H / R_{max} = 4$)

n	R_{min} / R_{max}	cylindrical		conical		barrel		hyperboloidal	
		$\rho\,(\text{kg/m}^3)$		$\rho\,(\text{kg/m}^3)$		$\rho\,(\text{kg/m}^3)$		$\rho\,(\text{kg/m}^3)$	
		7850	8300	7850	8300	7850	8300	7850	8300
3.5	0.4			300.1	291.9	248.2	241.3	330.4	321.4
	0.6			256.1	249.0	227.2	221.0	270.5	263.1
	0.8			213.1	207.3	202.6	197.0	220.0	213.9
	1.0	175.3	170.5	-	-	-	-	-	-
7.5	0.4			159.6	155.2	125.6	122.1	174.3	169.5
	0.6			130.4	126.8	114.2	111.1	136.4	132.6
	0.8			104.1	101.2	99.8	97.1	106.8	103.9
	1.0	84.5	82.1	-	-	-	-	-	-
11.5	0.4			106.2	103.3	82.8	80.5	114.8	111.7
	0.6			85.8	83.5	75.4	73.3	89.1	86.6
	0.8			68.2	66.3	65.6	63.8	69.8	67.9
	1.0	55.3	53.8	-	-	-	-	-	-

Table 10. continuing…
(b) B.C. (boundary condition): fixed-free ($R_{max} = 20\,\text{mm}$, $H / R_{max} = 4$)

n	R_{min} / R_{max}	cylindrical		conical		barrel		hyperboloidal	
		ρ(kg/m^3)		ρ(kg/m^3)		ρ(kg/m^3)		ρ(kg/m^3)	
		7850	8300	7850	8300	7850	8300	7850	8300
3.5	0.4			69.4	67.5	60.2	58.5	81.7	79.4
	0.6			60.7	59.0	55.5	53.9	66.9	65.1
	0.8			53.5	52.0	51.3	49.9	55.9	54.4
	1.0	47.5	46.2	-	-	-	-	-	-
7.5	0.4			33.4	32.5	28.7	27.9	39.5	38.5
	0.6			29.0	28.2	26.4	25.7	32.0	31.1
	0.8			25.4	24.7	24.3	23.6	26.6	25.8
	1.0	22.5	21.9	-	-	-	-	-	-
11.5	0.4			21.9	21.3	18.8	18.3	25.9	25.2
	0.6			19.0	18.4	17.2	16.8	20.9	20.4
	0.8			16.6	16.2	15.9	15.5	17.4	16.9
	1.0	14.7	14.3	-	-	-	-	-	-

4. CONCLUSION

The mixed finite element formulation is based on the Timoshenko beam theory, and the documentation of the corresponding functional exists in [7,8]. The non-cylindrical helix geometry is derived using exact curvatures at the nodal points and their interpolations through the element. As a convergence test, a barrel type helicoidal bar is handled, results of the present program is compared by the literature and a commercial program, and even with a coarse element mesh excellent agreement is achieved. In this study, four benchmark examples are solved to investigate the influence of the thickness-to-section average radius ratio, the helix height-to-helix maximum radius ratio, the various parameters of the non-cylindrical helicoidal geometry, the boundary conditions, and the density of the material on the free vibration analysis of helicoidal bars having thin-walled circular tube cross-section. Following remarks can be cited:

- As the thickness-to-section average radius ratio increases, an increasing trend is observed for the fundamental natural frequency.
- If the fundamental natural frequencies of the non-cylindrical helices are compared with the fundamental natural frequencies of the cylindrical helix, the latter is smaller.
- As the number of active turns and the ratio R_{min} / R_{max} increase, a reduction in the fundamental natural frequencies of the non-cylindrical helicoidal bars is observed.
- For both the cylindrical and non-cylindrical helicoidal bars, an increase of the density of material caused a reduction of the fundamental natural frequencies.

Acknowledgments / Teşekkür

This research is supported by The Scientific and Technological Research Council of Turkey under project no 111M308 and by the Research Foundation of ITU under project no 38078. These supports are gratefully acknowledged by the authors.

REFERENCES / KAYNAKLAR

[1] Michell JH, The small deformation of curves and surfaces with application to the vibrations of a helix and a circular ring, Messenger of Mathematics, 19:68-82, 1890.
[2] Love AEM, The propagation of waves of elastic displacement along a helical wire, Transactions of the Cambridge Philosophical Society, 18:364-374, 1899.
[3] Yoshimura Y and Murata Y, On the elastic waves propagated along coil springs, Institute of Science and Technology, Tokyo University, 6(1):27-35, 1952.
[4] Wittrick WH, On elastic wave propagation in helical spring, International Journal of Mechanical Science, 8:25-47, 1966.
[5] Lin Y and Pisano AP, General dynamic equations of helical springs with static solution and experimental verification, J. Appl. Mech., 54:910-917, 1987.
[6] Mottershead JE, Finite elements for dynamical analysis of helical rods, Int. J. Mech. Sci., 2(1):267-283, 1980.
[7] Omurtag MH and Aköz AY, The mixed finite element solution of helical beams with variable cross-section under arbitrary loading, Computers and Structures, 43(2):325-331, 1992.
[8] Girgin K, Free vibration analysis of non-cylindrical helices with, variable cross-section by using mixed FEM, Journal of Sound and Vibration, 297:931-945, 2006.
[9] Pearson D, The transfer matrix method for the vibration of compressed helical springs, Journal Mechanical Engineering Science, 24(4):163-171, 1982.
[10] Yıldırım V, Investigation of parameters affecting free vibration frequency of helical springs, Int. J. Num. Meth. Engng., 39(1):99-114, 1996.
[11] Yıldırım V and İnce N, Natural frequencies of helical springs of arbitrary shape, Journal of Sound and Vibration, 204(2):311-329, 1997.
[12] Yıldırım V, Free vibration analysis of non-cylindrical coil springs by combined use of the transfer matrix and complementary functions methods, Communications in Num. Meth. Engng., 13:487-494, 1997.
[13] Yıldırım V, A parametric study on the free vibration of non-cylindrical helical springs, Journal of Applied Mechanics, ASME, 65:157-163, 1998.
[14] Yıldırım V, Expressions for predicting fundamental natural frequencies of non-cylindrical helical springs, Journal of Sound and Vibration, 252(3):479-491, 2002.
[15] Busool W and Eisenberger M, Free vibration of helicoidal beams of arbitrary shape and variable cross section, Journal of Vibration and Acoustics, 124:397-409, 2002.
[16] Lee J, Free vibration analysis of cylindrical helical springs by the pseudospectral method, Journal of Sound and Vibration, 302:185-196, 2007.
[17] Lee J, Free vibration analysis of non-cylindrical helical springs by the pseudospectral method, Journal of Sound and Vibration, 305:543-551, 2007.
[18] Oden JT and Reddy JN, Variational Method in Theoretical Mechanics, Berlin: Springer-Verlag; 1976.
[19] Omurtag MH, Strength of Material 2, Istanbul: Birsen Press; 2013.